

Nano-Opto-Electro-Mechanical Systems

Leonardo Midolo¹, Albert Schliesser¹, and Andrea Fiore²

¹*Niels Bohr Institute, University of Copenhagen, Blegdamsvej 17, DK-2100 Copenhagen, Denmark*

²*Department of Applied Physics and Institute for Photonic Integration, Eindhoven University of Technology, PO Box 513, 5600 MB Eindhoven, The Netherlands*

Abstract

A new class of hybrid systems that couple optical, electrical and mechanical degrees of freedom in nanoscale devices is under development in laboratories worldwide. These nano-opto-electro-mechanical systems (NOEMS) offer unprecedented opportunities to dynamically control the flow of light in nanophotonic structures, at high speed and low power consumption. Drawing on conceptual and technological advances from the field of optomechanics, they also bear the potential for highly efficient, low-noise transducers between microwave and optical signals, both in the classical and quantum domains. This Progress Article discusses the fundamental physical limits of NOEMS, reviews the recent progress in their implementation, and suggests potential avenues for further developments in this field.

Introduction

Controlling light propagation is one of the most important challenges in optics and photonics, and has direct impact on optical communications (e.g. modulation, optical switching, device and network re-configurability), as well as sensing and imaging (e.g. beam steering). From the general laws of electromagnetism, it is clear that such control can be achieved either by a variation of the refractive index in a given medium, or by a displacement of the physical boundaries between media of different indices. The former is employed, e.g., in electro-optic modulators, whereas the latter is used for beam steering by macroscopic or microscopic mirrors. The refractive index tuning range, provided by the application of electric fields¹, strain², temperature³ or carrier injection⁴, is limited to $\Delta n = 10^{-3} - 10^{-2}$ in most materials, which often limits the applicability of these approaches. Additionally, the most effective tuning methods (such as temperature tuning and carrier injection) are inevitably associated with significant static power dissipation. In contrast, mechanical displacements can produce large effects (think of a turning mirror) and, in principle, require energy only for switching to a different state. Electrical actuation is readily obtained by exploiting electrostatic or piezoelectric forces. Miniaturization of motorized mirrors and other optical components has led to the development of micro-opto-electro-mechanical systems (MOEMS, or optical MEMS), which are at the heart of commercial technologies such as digital-light-processing (DLP) beamers and optical switches⁵.

The electrical actuation of a moving part within a light-confining structure (e.g. a waveguide or a cavity) can be used to tune the phase or frequency of the corresponding optical field, producing an effective electro-optic interaction (Fig. 1). Importantly, we note that this interaction is bi-directional because it is based on fundamentally reciprocal effects. In particular, light exerts forces, e.g., radiation pressure from an optical beam reflected off a mirror, which can induce displacement of a mechanically compliant object. Displacements, in turn, can induce voltages and currents in a piezoelectric material or a charged capacitive transducer. The field of optomechanics has intensely studied the intricate dynamics emerging from this coupling throughout the past decade⁶. While the initial focus has rested on one electromagnetic (i.e. optical or microwave) mode and one mechanical degree of freedom only, recent theoretical and experimental work has also brought out the potential of hybrid systems. In particular, the combination of optical, electronic and mechanical functionality enables a range of novel applications, ranging from electric tunability of optomechanical devices⁷, to the interconversion of microwave and optical quantum signal, as required to connect superconducting

quantum circuits into a network. Conversion via mechanical intermediaries is attractive, given the realistic prospect to reach unity efficiency and near-zero noise temperature^{8–14}, which poses a challenge to competing technologies such as direct electro-optic conversion^{15–17} or magnonic transducers^{18–20}.

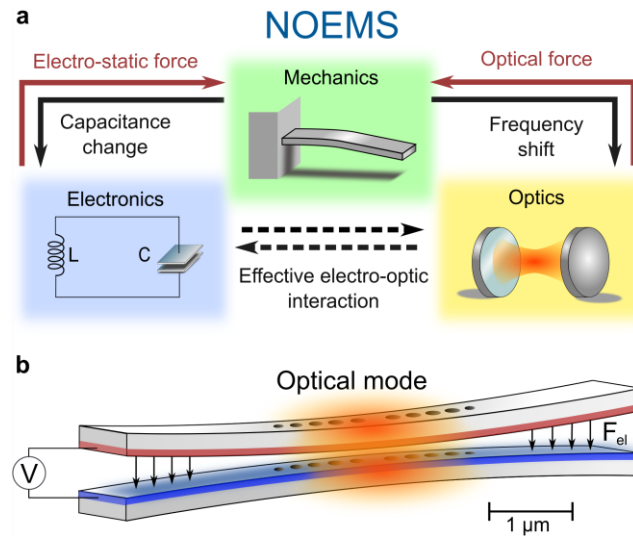


Figure 1: Physics of nano-opto-electromechanical systems. (a) NOEMS combine electronics, mechanics, and optics. Direct and inverse effects between these three degrees of freedom are mediated by mechanical deformations. In particular, NOEMS allow enhancing electro-optical effects through mechanical degrees of freedom. (b) Artistic view of a NOEMS. Electrostatic forces between two electrodes and optical forces in coupled sub-wavelength waveguides couple charges, mechanical displacement and the optical field.

Taking such systems to the nanoscale—that is, confining electromagnetic and displacement fields to sub-micrometer dimensions—offers opportunities for dramatically enhanced interaction strength, increased bandwidth, lower power consumption, and chip-scale fabrication and integration. These prospects have triggered a mobilization of both nanophotonics and optomechanics communities towards the realization of such nano-opto-electro-mechanical systems (NOEMS, Fig. 1), in spite of the associated technological challenges. In this Progress Article, we review recent progress in this burgeoning field, with a particular emphasis on the underlying fundamentals, the physical limits to miniaturization and speed they imply, and a representative set of particularly promising applications. Given the large body of activity in this field, we choose to restrict the scope of this article to structures that exploit nanoscale light localization in waveguides and cavities, and refer the reader interested in electrically actuated metamaterials and metasurfaces to another recent review²¹.

Fundamentals of NOEMS

In many photonic materials, the interaction between electrical, mechanical and optical degrees of freedom determines some of the intrinsic properties of solids. For example, the deformation of the atomic lattice under an applied electric field (inverse piezoelectric effect) produces a change in refractive index (photoelastic effect) and thereby contributes to the electro-optic effect. The bulk electro-optic effect depends on the material, but is typically weak in semiconductors and in particular absent in centrosymmetric materials as silicon. NOEMS are structures designed to simultaneously maximize the opto-mechanical and electro-mechanical interaction at the nanoscale. They are based on nanomechanical structures optimized to respond maximally to an applied electrical force and produce a strong effect on a co-located optical field either through the displacement of their boundaries or through the photoelastic effect (see Box 1). An important example is the case of two parallel and evanescently-coupled nanophotonic waveguides (see Box 2) supporting optical modes whose propagation constant depends on the distance between the waveguides and can be actuated

electrostatically. Due to the possibility of designing the electro-mechanical and opto-mechanical coupling (Box 1) and the stiffness, such an effective medium can exhibit a strong electro-optic effect regardless of the physical properties of the material of which it is constituted.

A major drive towards reducing opto-electro-mechanical systems to smaller dimensions is given by the fact that opto-electro-mechanical effects become more sizeable at these scales enabling novel applications in sensing, signal transduction, and optical routing in a wide range of materials, independent of their intrinsic electro-optic coefficient. Optical forces and, in particular, gradient forces²², become relevant only in the presence of wavelength-scale confinement and strong gradients of the field, particularly in nano-holes or slots. Similarly, electrostatic forces scale inversely with the square of the charge separation, so that the requirement for high voltage drives is reduced for sub- μm electrode spacing (the actuation voltages for the NOEMS considered here can be reduced to few Volts). Additionally these spacings are shorter than the average distance between electron collisions in air, which allows capacitors to operate without incurring in electrostatic discharges²³, the maximum voltage being ultimately limited by field emission or electromechanical instabilities known as pull-in effect²⁴.

Another advantage of NOEMS with respect to bulk piezo-electric and photoelastic effects is the possibility to engineer the mechanical response. In the presence of distributed forces, a solid system responds with a deformation which is linear for small deformations (strain within few percent), which holds in most practical situations for crystalline solids. Notwithstanding the complexity of a full three-dimensional displacement function, a generalized Hooke's law of the type $F = kx$ can always be defined for a specific spatial coordinate and a specific load distribution. For simple structures such as cantilevers and doubly-clamped beams, the reduced stiffness k (units of N/m) scales as $\propto EI/L^3$, where E is the Young modulus (a material property), I the moment area of inertia (units of m^4) and L the length of the structure. This implies that the stiffness scales linearly when the size of the object is uniformly scaled²¹. When at least one dimension is sub- μm (as in nano-membranes or nano-wires), a spring constant in the order of 1 N/m is easily achievable. Such stiffness is sufficiently low to reach displacements in the order of several tens of nm and, correspondingly, large optical effects with forces in the nN- μN range. These forces are routinely achieved in sub-micrometer capacitive, or electrostatic, actuators.

NOEMS therefore offer a powerful way to engineer and enhance electro-optic effects in nanophotonic devices. We should, however, mention some notable differences between the electro-optic effect and NOEMS. One important aspect is the response time achievable in these two systems. The electronic response to applied fields is nearly instantaneous so that electro-optic devices are easily operated at frequencies of 10's of GHz. This fact is widely exploited for Gb/s data encoding in telecommunication. The electro-mechanical actuation instead, is ultimately limited in speed by the mechanical susceptibility, characterized by a cut-off at the fundamental resonance frequency $\omega = \sqrt{k/m_{eff}}$ where m_{eff} is the effective mass. This represents the equivalent mass that a mechanical mode would have if it were treated as a simple mass-spring system. As for a given force the stiffness is proportional to the displacement, the only solution to achieve faster motion without sacrificing the actuation is to scale the size of the structure (the mass reduces with a third power law, yielding a linear reduction of frequency). Downscaling the structure to sub- μm dimensions allows reducing the switching time to the sub- μs level, well below the ms timescale typical of MEMS. Reaching GHz frequencies requires further scaling the devices to sub-pg masses. This would involve photonic structures with moving parts with dimensions of few tens of nm, and correspondingly a field confinement at these scales, which, for typical near-infrared wavelengths, can only be achieved in plasmonic structures^{25,26} or in slotted photonic crystals^{27,28}. If repetitive or periodic operation is possible, higher-order modes and resonant driving can be used to reach higher actuation speeds. The mechanical resonances will greatly amplify the motion. Resonant operation is often implemented in Pockels cells to reduce the required driving voltage and to realize pulse-picking and spatial demultiplexing. Additionally, resonances could be exploited for enhancing the electro-mechanical and opto-mechanical coupling, which is crucial in sensing and signal transduction applications.

Applications to light control and switching

Several applications of NOEMS in nanophotonics have recently emerged, in particular for switching, routing, and phase-shifting in integrated photonic circuits. While commercial electro-optic and acousto-optic devices provide very fast (picoseconds to nanoseconds) modulation speeds for data encoding in telecommunications, NOEMS are expected to play a more important role for static and microsecond-scale re-configuration of optical circuits. The main advantages for using mechanics, rather than more conventional electro-optic or thermo-optic effects, are reduced losses, small device footprints, and low-power consumption. Early attempts of using electromechanical actuation for switching relied on controlling the relative alignment between waveguides²⁹ and sliding reflective structures³⁰. These methods however require relatively large displacements (in the range of several μm) and therefore large and complex actuating structures and high applied voltage.

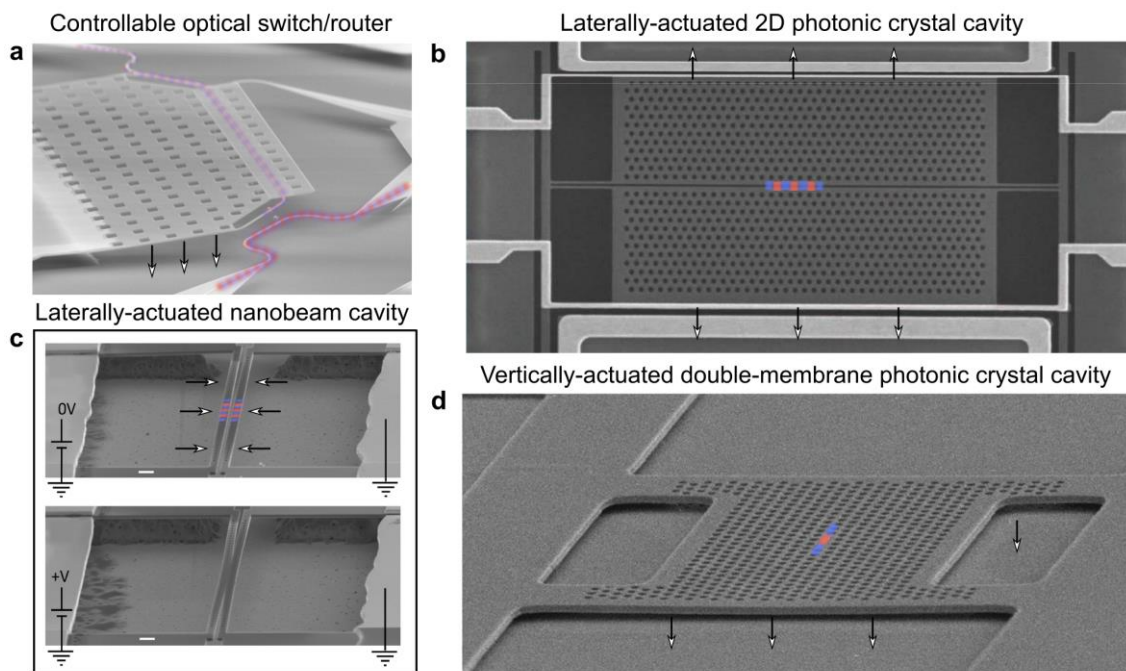


Figure 2. Examples of NOEMS applications. (a) Controllable optical switch based on micro-electro-mechanical actuation³¹. Light is routed by out-of-plane motion of directional couplers attached to a cantilever. (b) An electro-opto-mechanical cavity based on slot waveguides suitable for microwave-to-optical conversion^{32,33}. Lateral electrostatic actuators with <50 nm air gaps allow a large wavelength shifts due to the extremely high sensitivity of photonic nanostructures to nano-slots. (c) A programmable photonic crystal cavity made of two electrostatically-actuated nanobeams³⁴. (d) Vertically-actuated 2D photonic crystal cavity on GaAs with embedded quantum emitters³⁵. The direction of the electrostatic field (black arrows) and an artistic representation of the optical field have been overlaid on each figure.

Recently, the attention has shifted to the control of the evanescent coupling between two optical modes (e.g. in two nearby waveguides) by changing their distance^{26,36,37}. This relatively simple architecture can be tailored to obtain a plethora of effects, which become stronger in nanophotonic structures due to the large evanescent fields. The simplest, and probably most intuitive, is the change of the propagation constant of the supermodes due to the evanescent coupling (see Box 2).

Experimental demonstrations of MEMS-based switching on silicon have been reported using in-plane motion of directional couplers³⁸ or ring resonator geometries³⁹. Recently, Han et al.³¹ and Seok et al.⁴⁰ have demonstrated networks of thousands of optical switches based on Silicon directional couplers or adiabatic couplers mounted on electro-mechanical cantilevers (see Fig. 2a) where each switch has very low loss. These examples, although they still involve relatively large micro-mechanical actuators and can therefore be considered as MEMS, demonstrate the great potential of opto-electro-mechanical systems for realizing low-loss networks of switches with MHz-range bandwidth. Moreover they

provide interesting solutions and concepts that could be further scaled down in size and optimized for speed. This has been shown by Poot et al⁴¹ using a more compact design of electrodes, where a nano-electro-mechanical phase shifter on SiN waveguides with sub- μ s speed has been reported, while a nanomechanical 2x2 switch design with very small actuation voltage and interaction length has been proposed by Liu et al⁴². The next frontier in optical switching will require ~ 10 ns response times for packet switching. Aggressively scaled nanomechanical systems may manage to achieve these time scales, which would make likely candidates for the switching fabrics in high-performance data center networks.

In the cases discussed above the dispersion relation is still, to good approximation, linear and therefore no group effects are employed. When the dispersion is modified to provide slow-light effects, or optical band-gaps, as in photonic crystals, the mechanical switching can have a dramatic effect on waves with frequencies close to band edges or to a localised resonance. The combination of photonic crystal nano-cavities and nanomechanics has in fact attracted much attention in the recent years. Research in opto-mechanics engineers very strong dispersive couplings $d\omega/dx$ (see Box 1) in order to enhance radiation pressure, but can also realise higher-order coupling ($\omega \propto x^2$) as required for some sensing protocols⁴³. Several works have shown electromechanically-tunable PhC cavities using side-coupled nanowire cavities^{34,44-47}, slot waveguides³², or double-membrane cavities⁴⁸. Some examples are shown in Fig. 2b, 2c, and 2d. Record tuning ranges of up to 30 nm have been obtained with few V applied bias and negligible power dissipation, showing the full potential of electromechanical tuning⁴⁹.

Recently, some new applications of mechanical actuation have been explored. Among these, the (electro)mechanical tuning of a photonic structure “on the fly” (i.e. within the photon lifetime) has been proposed as a means to realize frequency conversion⁵⁰ and indeed piezoelectric tuning of a waveguide during a single photon’s transit can shift the photon’s frequency by up to 150 GHz while preserving coherence⁵¹. Further, rather than controlling the frequency of an optical mode, its optical loss and quality factor can be altered by mechanically modifying the cavity structure⁵² or controlling the coupling rate with an output channel such as a waveguide⁵³⁻⁵⁵. This “dissipative coupling” has been studied in the field of optomechanics as an alternative to the usual dispersive coupling approach⁵⁶, and its electrical control could lead to Q-switched semiconductor lasers and generally to improved control of filters. More generally, a mechanical reconfiguration can be used to modify the field distribution of the cavity mode, leading to modified radiative interactions with integrated quantum emitters⁵⁷.

As discussed above, one of the main strength of NOEMS is their compactness and, consequently, the low insertion loss and low power consumption. The benefits of preferring a nano-mechanical approach for optical reconfiguration or switching becomes even more evident in situations where optical amplification is not possible and low-power operation is needed. This is the case, for example, of quantum photonic networks, where the manipulation and routing of single photons (e.g. for boson sampling⁵⁸ and quantum simulation⁵⁹) requires reconfigurable architectures, composed of single-photon sources, beam-splitters, phase shifters and detectors. Especially when sources or detectors are integrated on the chip, these circuits require cryogenic operation (< 10 K). As thermo-optic tuning cannot be used at such temperatures and carrier injection produces heating and spurious photon emission, NOEMS are expected to play a key role in quantum photonic networks.

Applications to signal transduction

In addition to electro-mechanical switching or re-routing of optical signals, the effective electro-optical interaction in NOEMS is also very promising for the direct transduction of signals between the electrical and optical domains, using the mechanics as intermediary. In contrast to coupling via bulk optical nonlinearities, this coupling can be enhanced by tailored mechanical mode shapes, in particular at the nanoscale, as already alluded to above.

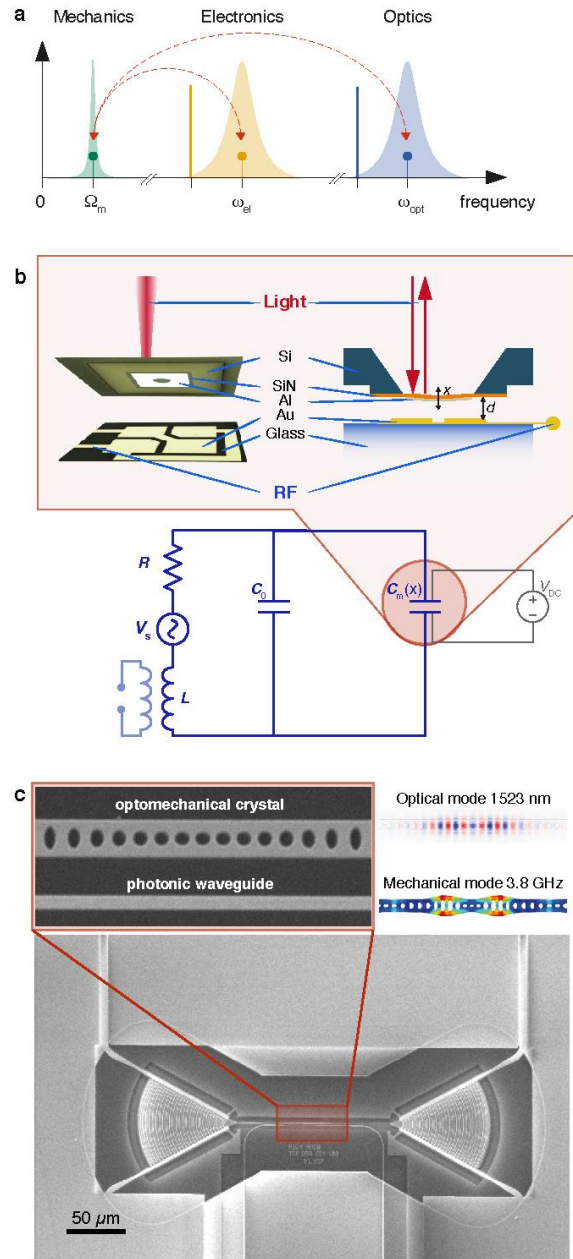


Figure 3. Opto-electro-mechanical signal transducers. (a) Generic all-resonant signal transducer, coupling excitations (thin lines with disk tip) of a mechanical, electronic, and optical resonance, indicated by green, yellow and blue Lorentzians, respectively. Parametric coupling (dashed red lines) is enhanced by biasing fields (bold yellow and blue lines), tuned to the difference frequency of the electromagnetic (electronic or optical) and mechanical mode. (b) Electro-opto-mechanical transducer for classical radio-frequency signals⁶⁰ based on a silicon nitride (SiN) membrane, forming a mechanically compliant capacitor $C_m(x)$. Together with a tuning capacitor C_0 , and an inductor it forms an RF resonant circuit, in this case degenerate with the mechanical mode, $\omega_{el}=\Omega_m$. Correspondingly, the biasing field is a d.c. voltage. In this proof-of-principle experiment, the optical readout is non-resonant. (c) Piezoelectric optomechanical crystal for bidirectional microwave–optical quantum signal conversion⁶¹. A pair of radially symmetric interdigitated transducers launches Lamb waves, via direct piezoelectric coupling of the signal’s microwave field and the strain in the device’s AlN material. The waves travel towards an optomechanical crystal, which hosts both high quality mechanical and optical modes. The latter can be driven and read out with an optical bias field provided by an evanescently coupled photonic waveguide.

Two different regimes of operation can be distinguished, depending on whether a resonance is employed in the electrical and/or mechanical domain (e.g. through the use of an LC circuit). Non-resonant operation can allow the optical detection of electrical signals or charges in a broad frequency range, namely up to the lowest mechanical frequency, which can be in the MHz to 100s MHz range. As a simple illustration, a single electron in a nano-opto-electromechanical PhC cavity produces forces in the fN range, which can be detected optically⁶². This makes NOEMS sensors potentially more sensitive to charge than conventional solid-state electrometers. The sensitivity to electric fields can be boosted by using resident charges (e.g. in the depletion region of a p-i-n junction⁴⁸) to increase the electrostatic force. Optical sensing of electric signals with NOEMS can therefore feature high sensitivity and spatial resolution, and may be particularly relevant in applications where tiny charges must be measured (for example for the detection of ionizing radiation), or where direct electrical read-out is difficult due to electromagnetic interference – for example in electric transmission lines and generators.

Exploiting resonances—both electromagnetic (EM) and mechanical—can dramatically boost the coupling, in particular in conjunction with biasing fields. In the common setting of a parametric coupling, in which mechanical displacements modulate the EM resonance frequencies, the coupling is enhanced: the coupling rate, at which elementary photon-phonon conversion takes place⁶, is given by $g = \frac{d\omega}{dx} x_0 \bar{a}$, where \bar{a} is the mean field (normalised such that $|\bar{a}|^2$ is the number of photons in the EM resonator), and $x_0 = \sqrt{\frac{\hbar}{2m\Omega_m}}$ the mechanical mode's zero-point motion. Simultaneously, the biasing fields can fulfil a second crucial role: matching their oscillation frequencies with the differences (or also sums) of mechanical and optical—or electronic—resonance frequencies, renders the parametric coupling effectively resonant, even though the subsystems (optical, mechanical, electronic) reside in very different frequency regimes (100's of THz, MHz, GHz). In a simple picture, a signal conversion process (Fig. 3a) consists of two steps: A microwave cavity photon is converted to the detuned microwave pump frequency through the emission of a phonon. The latter is then upconverted to the optical cavity, assisted by an optical pump photon. This scheme^{8–13} extends the coupled photon-phonon dynamics championed by the field of optomechanics⁶.

In the ultimate limit, such transducers can be bidirectional and noise-free, enabling high-fidelity conversion of quantum states from the microwave to the optical domain and back¹⁴. Such a hybrid quantum interface is a crucial, and yet missing, ingredient for networks that connect superconducting qubit processors via optical links^{63,64}. The ideal, internal conversion efficiency¹⁴ $\eta = \frac{4C_e C_o}{(C_e + C_o + 1)^2}$ of such a transducer is governed by the electro- and optomechanical cooperativities $C_{e/o} = \frac{4g_{e/o}^2}{\kappa_{e/o}\Gamma_m}$, and approaches unity for $1 \ll C_e = C_o \equiv C$. This reflects the competition of couplings $g_{e/o}$ with the loss rates $(\kappa_e, \kappa_o, \Gamma_m)$ of the electric, optical, and mechanical resonators, respectively—but also an impedance-matching condition, favouring matched conversion ($C_e = C_o$). In addition, the mechanics is linked to a thermal bath with a large mean occupation $\bar{n}_{th} \approx k_B T / \hbar \Omega_m$ via its dissipation. The corresponding thermal fluctuations leak into the converter output, resulting in $N \approx \bar{n}_{th} / C \equiv 1 / C_q$ noise quanta (per bandwidth per time), where C_q is referred to as the quantum cooperativity. Thus for both key figures of merit, efficiency η and added noise N , high coupling rates $g_{e/o}$ and small mechanical dissipation Γ_m are desirable. A full analysis must further account for external coupling losses (at the input and output of the electromagnetic resonators), added quantum noise due to insufficiently resolved motional sidebands (i.e. if $\kappa_e, \kappa_o \ll \Omega_m$ cannot be reached), and the resulting performance trade-offs⁶⁵.

An early experiment demonstrated measurement of radio-frequency voltage signals via a mechanically resonant membrane transducer⁶⁰ whose electrostatically induced out-of-plane motion was detected with a shot-noise-limited laser interferometer (Fig. 3b). Remarkably, it achieved room-temperature voltage sensitivity (<1 nV/ $\sqrt{\text{Hz}}$) and noise temperature (<20 K) competitive with state-of-the-art electronic amplifiers [61]. Much improved noise performance could be achieved if electronic Johnson noise in the input is reduced; thermomechanical noise and the quantum noise of light (the

ultimate limit) add as little as ($<60 \text{ pV}/\sqrt{\text{Hz}}$) each. Integrated devices of this kind could therefore transduce nV-level electric signals—for example, from a magnetic resonance coil⁶⁶—directly to an optical field that propagates with low loss and cross-talk on an optical fibre. The reverse conversion from optical to microwave has also been demonstrated recently⁶⁷.

Andrews *et al.*⁶⁸ have shown bidirectional, overall 10%-efficient microwave-optical conversion with $\sim 10^3$ added noise quanta. This system is also based on a SiN membrane, here coupled capacitively to a superconducting LC circuit, and via radiation-pressure with the optical photons in a Fabry-Pérot resonator. Operation at lower temperature, or with more coherent mechanical devices⁶⁹, could bring a quantum-enabled transducer into reach. Efforts to downscale such devices are underway in several groups worldwide, promising not only larger coupling rates, but also all-nanofabricated, scalable platforms. For example, working with in-plane mechanical modes of silicon^{32,33} or silicon nitride⁷⁰ membranes allows the definition and alignment of capacitor electrodes, mechanical structure and optical nanoresonator with nm-scale precision. Sub-100 nm capacitive gaps can be realised in this manner, enabling record coupling rates if parasitic (not mechanically compliant) capacitance is kept at bay.

Piezoelectric coupling again provides interesting design alternatives⁷¹ as even high-frequency modes can be efficiently driven without the need to define an electromechanical capacitor. Optomechanical whispering gallery-mode resonators⁷² in the piezoelectric AlN^{73,74} have been used for early work, followed by several implementations building on optomechanical crystals²⁷ in the same material. Bidirectional microwave-optical conversion can be achieved by launching GHz surface acoustic waves from an interdigitated transducer^{61,75–79} (see Fig. 3c). To date, however, demonstrated “internal” conversion efficiencies are only at the percent level, and lower (order 10^{-4}) if all in- and output losses are considered^{61,75}. Increasing internal efficiency might necessitate a boost in optomechanical coupling, which can hardly come from variations of the highly optimised geometry. It is available in GaAs optomechanical crystals, though, where photoelastic interaction contributes significantly to record-high optomechanical coupling^{77,80}. A smaller piezoelectric coefficient is the price to pay in this case, which has, as yet, precluded bidirectional operation with noteworthy efficiency.

From the above examples it is evident that quantum transducers pose extreme demands to the devices’ materials and design—even to work in principle, not to mention such practicalities as absorption heating in milliKelvin environments⁸¹. Yet, it is clear that mechanical transducers are highly promising contenders, given the successes already demonstrated, and known routes for improvement. Direct integration of phononic modes with microwave qubits could improve efficiency in optically addressing the latter^{82,83}. Advanced protocols can circumvent challenging requirements such as the resolved-sideband regime⁸⁴. And more options exist for the delicate choice of materials, including large-bandgap piezoelectrics such as GaP. It will be exciting to see the development of these systems, and their performance compared to complementary approaches such as those based on direct electro-optic conversion^{15–17} and magnon transducers^{18–20}, which rely on spin waves in ferrimagnets such as Yttrium iron garnet (YIG), as intermediary mode instead of a mechanical one. As yet however, their conversion efficiencies have remained below the 1%-mark.

Beyond the examples discussed above, a wide range of opportunities has yet to be explored. For example, reservoir engineering or modulation schemes can render signal transport across the microwave and optical spectral domains non-reciprocal^{85–87}. This will allow on-chip implementation of isolators and circulators, without the need for magnetic materials. Passive microwave photonic devices, such as filters or delay lines, can be implemented on-chip—with a compact footprint, exploiting the much shorter ($\sim 10^{-5}$) wavelength of phonons compared to electromagnetic waves of the same frequency^{80,88}. Optically pumped active devices can eventually lead to a new generation of chip-scale microwave oscillators with high spectral purity, as required for advanced communications and radar applications⁸⁹.

Outlook

The strong effective electro-optic coupling achievable through the nanoscale co-localization of charges, mechanical motion and optical fields makes NOEMS unique contenders for a wide range of applications in communication, sensing and quantum information processing. Progress in theoretical understanding, device design and nanofabrication methods enables the demonstration of increasing functional and efficient structures, ranging from reconfigurable devices and circuits, to fast optical switches, optical sensors and signal transducers. On the route towards turning such concepts into real-world, mass-producible devices, much will hinge on the successful development of suited materials and processes, compatible with CMOS and foundry-level fabrication. In particular, NOEMS pose stringent requirements in the lithography, for resolution and alignment accuracy (both within tens of nm) of nanophotonic structures. While this is mostly achieved by electron-beam lithography in research demonstrators, deep-UV lithography within CMOS foundries has also been shown to enable high-quality optomechanical structures⁹⁰, and should be applicable for NOEMS as well. Packaging, too, will have to be addressed, given that mechanical systems require isolation from the environment. Such isolation can in many cases be achieved by hermetic sealing to avoid moisture damage (oxidation, corrosion and adhesion of suspended parts). For applications such as coherent signal transduction, where high mechanical quality factors are important (e.g. to minimize squeeze-film damping), packaging in vacuum is required⁹¹. While such chip-scale MEMS packaging technology is currently available (in particular for inertial sensors), the combination with precise optical alignment (chip-to-fiber interfaces, pigtailed) is required and may pose additional challenges. Yet, with a number of major industrial players in the field of microelectronics and MEMS joining this line of research, the prospects are now better than ever.

References

1. Liu, K., Ran Ye, C., Khan, S. & Sorger, V. J. Review and perspective on ultrafast wavelength-size electro-optic modulators - Liu - 2015 - Laser & Photonics Reviews - Wiley Online Library. Available at: <http://onlinelibrary.wiley.com/doi/10.1002/lpor.201400219/full>. (Accessed: 6th April 2017)
2. Baker, C. *et al.* Photoelastic coupling in gallium arsenide optomechanical disk resonators. *Opt. Express* **22**, 14072–14086 (2014).
3. Faraon, A. & Vučković, J. Local temperature control of photonic crystal devices via micron-scale electrical heaters. *Appl. Phys. Lett.* **95**, 043102-043102-3 (2009).
4. Bennett, B. R., Soref, R. A. & Del Alamo, J. A. Carrier-induced change in refractive index of InP, GaAs and InGaAsP. *IEEE J. Quantum Electron.* **26**, 113–122 (1990).
5. Motamedi, M. E. *MOEMS: Micro-opto-electro-mechanical Systems*. (SPIE Press, 2005).
6. Aspelmeyer, M., Kippenberg, T. J. & Marquardt, F. Cavity optomechanics. *Rev. Mod. Phys.* **86**, 1391–1452 (2014).
7. Miao, H., Srinivasan, K. & Aksyuk, V. A microelectromechanically controlled cavity optomechanical sensing system. *New J. Phys.* **14**, 075015 (2012).
8. Regal, C. A. & Lehnert, K. W. From cavity electromechanics to cavity optomechanics. *J. Phys. Conf. Ser.* **264**, 012025 (2011).
9. Safavi-Naeini, A. H. & Painter, O. Proposal for an optomechanical traveling wave phonon–photon translator. *New J. Phys.* **13**, 013017 (2011).
10. Taylor, J. M., Sørensen, A. S., Marcus, C. M. & Polzik, E. S. Laser Cooling and Optical Detection of Excitations in a LC Electrical Circuit. *Phys. Rev. Lett.* **107**, 273601 (2011).
11. Barzanjeh, S., Abdi, M., Milburn, G. J., Tombesi, P. & Vitali, D. Reversible Optical-to-Microwave Quantum Interface. *Phys. Rev. Lett.* **109**, 130503 (2012).
12. Wang, Y.-D. & Clerk, A. A. Using Interference for High Fidelity Quantum State Transfer in Optomechanics. *Phys. Rev. Lett.* **108**, 153603 (2012).
13. Tian, L. Adiabatic State Conversion and Pulse Transmission in Optomechanical Systems. *Phys. Rev. Lett.* **108**, 153604 (2012).
14. Tian, L. Optoelectromechanical transducer: Reversible conversion between microwave and optical photons. *Ann. Phys.* **527**, 1–14 (2015).

15. Javerzac-Galy, C. *et al.* On-chip microwave-to-optical quantum coherent converter based on a superconducting resonator coupled to an electro-optic microresonator. *Phys. Rev. A* **94**, 053815 (2016).
16. Rueda, A. *et al.* Efficient microwave to optical photon conversion: an electro-optical realization. *Optica* **3**, 597–604 (2016).
17. Tsang, M. Cavity quantum electro-optics. *Phys. Rev. A* **81**, 063837 (2010).
18. Haigh, J. A., Nunnenkamp, A., Ramsay, A. J. & Ferguson, A. J. Triple-Resonant Brillouin Light Scattering in Magneto-Optical Cavities. *Phys. Rev. Lett.* **117**, 133602 (2016).
19. Hisatomi, R. *et al.* Bidirectional conversion between microwave and light via ferromagnetic magnons. *Phys. Rev. B* **93**, 174427 (2016).
20. Zhang, X., Zhu, N., Zou, C.-L. & Tang, H. X. Optomagnonic Whispering Gallery Microresonators. *Phys. Rev. Lett.* **117**, 123605 (2016).
21. Zheludev, N. I. & Plum, E. Reconfigurable nanomechanical photonic metamaterials. *Nat. Nanotechnol.* **11**, 16–22 (2016).
22. Van Thourhout, D. & Roels, J. Optomechanical device actuation through the optical gradient force. *Nat. Photonics* **4**, 211–217 (2010).
23. Peschot, A., Bonifaci, N., Lesaint, O., Valadares, C. & Poulain, C. Deviations from the Paschen’s law at short gap distances from 100 nm to 10 μm in air and nitrogen. *Appl. Phys. Lett.* **105**, 123109 (2014).
24. Zhang, W.-M., Yan, H., Peng, Z.-K. & Meng, G. Electrostatic pull-in instability in MEMS/NEMS: A review. *Sens. Actuators Phys.* **214**, 187–218 (2014).
25. Thijssen, R., Verhagen, E., Kippenberg, T. J. & Polman, A. Plasmon Nanomechanical Coupling for Nanoscale Transduction. *Nano Lett.* **13**, 3293–3297 (2013).
26. Dennis, B. S. *et al.* Compact nanomechanical plasmonic phase modulators. *Nat. Photonics* **9**, 267–273 (2015).
27. Eichenfield, M., Chan, J., Camacho, R. M., Vahala, K. J. & Painter, O. Optomechanical crystals. *Nature* **462**, 78–82 (2009).
28. Leijssen, R. & Verhagen, E. Strong optomechanical interactions in a sliced photonic crystal nanobeam. *Sci. Rep.* **5**, 15974 (2015).
29. Pruessner, M. W. *et al.* End-coupled optical waveguide MEMS devices in the indium phosphide material system. *J. Micromechanics Microengineering* **16**, 832 (2006).
30. Lee, M.-C. M., Hah, D., Lau, E. K., Toshiyoshi, H. & Wu, M. MEMS-actuated photonic crystal switches. *IEEE Photonics Technol. Lett.* **18**, 358–360 (2006).
31. Han, S., Seok, T. J., Quack, N., Yoo, B.-W. & Wu, M. C. Large-scale silicon photonic switches with movable directional couplers. *Optica* **2**, 370 (2015).
32. Winger, M. *et al.* A chip-scale integrated cavity-electro-optomechanics platform. *Opt. Express* **19**, 24905–24921 (2011).
33. Pitanti, A. *et al.* Strong opto-electro-mechanical coupling in a silicon photonic crystal cavity. *Opt. Express* **23**, 3196–3208 (2015).
34. Frank, I. W., Deotare, P. B., McCutcheon, M. W. & Loncar, M. Programmable photonic crystal nanobeam cavities. *Opt. Express* **18**, 8705–8712 (2010).
35. Midolo, L. & Fiore, A. Design and Optical Properties of Electromechanical Double-Membrane Photonic Crystal Cavities. *IEEE J. Quantum Electron.* **50**, 404–414 (2014).
36. Van Acoleyen, K. *et al.* Ultracompact Phase Modulator Based on a Cascade of NEMS-Operated Slot Waveguides Fabricated in Silicon-on-Insulator. *IEEE Photonics J.* **4**, 779–788 (2012).
37. Pruessner, M. W., Park, D., Stievater, T. H., Kozak, D. A. & Rabinovich, W. S. Broadband opto-electro-mechanical effective refractive index tuning on a chip. *Opt. Express* **24**, 13917–13930 (2016).
38. Akihama, Y. & Hane, K. Single and multiple optical switches that use freestanding silicon nanowire waveguide couplers. *Light Sci. Appl.* **1**, e16 (2012).
39. Takahashi, K., Kanamori, Y., Kokubun, Y. & Hane, K. A wavelength-selective add-drop switch using silicon microring resonator with a submicron-comb electrostatic actuator. *Opt. Express* **16**, 14421 (2008).

40. Seok, T. J., Quack, N., Han, S., Muller, R. S. & Wu, M. C. Large-scale broadband digital silicon photonic switches with vertical adiabatic couplers. *Optica* **3**, 64–70 (2016).
41. Poot, M. & Tang, H. X. Broadband nanoelectromechanical phase shifting of light on a chip. *Appl. Phys. Lett.* **104**, 061101 (2014).
42. Liu, T., Pagliano, F. & Fiore, A. Nano-opto-electro-mechanical switch based on a four-waveguide directional coupler. *Opt. Express* **25**, 10166–10176 (2017).
43. Paráiso, T. K. *et al.* Position-Squared Coupling in a Tunable Photonic Crystal Optomechanical Cavity. *Phys. Rev. X* **5**, 041024 (2015).
44. Deotare, P. B., McCutcheon, M. W., Frank, I. W., Khan, M. & Lončar, M. Coupled photonic crystal nanobeam cavities. *Appl. Phys. Lett.* **95**, 031102-031102-3 (2009).
45. Perahia, R., Cohen, J. D., Meenehan, S., Alegre, T. P. M. & Painter, O. Electrostatically tunable optomechanical “zipper” cavity laser. *Appl. Phys. Lett.* **97**, 191112-191112–3 (2010).
46. Chew, X., Zhou, G., Chau, F. S. & Deng, J. Nanomechanically Tunable Photonic Crystal Resonators Utilizing Triple-Beam Coupled Nanocavities. *IEEE Photonics Technol. Lett.* **23**, 1310–1312 (2011).
47. Midolo, L. *et al.* Electromechanical tuning of vertically-coupled photonic crystal nanobeams. *Opt. Express* **20**, 19255–19263 (2012).
48. Midolo, L., van Veldhoven, P. J., Düндar, M. A., Nötzel, R. & Fiore, A. Electromechanical wavelength tuning of double-membrane photonic crystal cavities. *Appl. Phys. Lett.* **98**, 211120-211120–3 (2011).
49. Zobenica, Z. *et al.* Fully integrated nano-opto-electro-mechanical wavelength and displacement sensor. in *Advanced Photonics 2016 (IPR, NOMA, Sensors, Networks, SPPCom, SOF) (2016)*, paper SeW2E.4 SeW2E.4 (Optical Society of America, 2016). doi:10.1364/SENSORS.2016.SeW2E.4
50. Notomi, M., Taniyama, H., Mitsugi, S. & Kuramochi, E. Optomechanical Wavelength and Energy Conversion in High-Q Double-Layer Cavities of Photonic Crystal Slabs. *Phys. Rev. Lett.* **97**, 023903 (2006).
51. Fan, L. *et al.* Integrated optomechanical single-photon frequency shifter. *Nat. Photonics* **10**, 766–770 (2016).
52. Shi, P., Du, H., Chau, F. S., Zhou, G. & Deng, J. Tuning the quality factor of split nanobeam cavity by nanoelectromechanical systems. *Opt. Express* **23**, 19338–19347 (2015).
53. Yao, J., Leuenberger, D., Lee, M.-C. M. & Wu, M. C. Silicon Microtoroidal Resonators With Integrated MEMS Tunable Coupler. *IEEE J. Sel. Top. Quantum Electron.* **13**, 202–208 (2007).
54. Ohta, R. *et al.* Electro-Mechanical Q Factor Control of Photonic Crystal Nanobeam Cavity. *Jpn. J. Appl. Phys.* **52**, 04CG01 (2013).
55. Cotrufo, M. *et al.* Active control of the vacuum field in nanomechanical photonic crystal structures. in *Frontiers in Optics 2016 (2016)*, paper FTu3D.7 FTu3D.7 (Optical Society of America, 2016). doi:10.1364/FIO.2016.FTu3D.7
56. Elste, F., Girvin, S. M. & Clerk, A. A. Quantum Noise Interference and Backaction Cooling in Cavity Nanomechanics. *Phys. Rev. Lett.* **102**, 207209 (2009).
57. Cotrufo, M., Fiore, A. & Verhagen, E. Coherent Atom-Phonon Interaction through Mode Field Coupling in Hybrid Optomechanical Systems. *Phys. Rev. Lett.* **118**, 133603 (2017).
58. Wang, H. *et al.* High-efficiency multiphoton boson sampling. *Nat. Photonics* **advance online publication**, (2017).
59. Aspuru-Guzik, A. & Walther, P. Photonic quantum simulators. *Nat. Phys.* **8**, 285–291 (2012).
60. Bagci, T. *et al.* Optical detection of radio waves through a nanomechanical transducer. *Nature* **507**, 81–85 (2014).
61. Vainsencher, A., Satzinger, K. J., Peairs, G. A. & Cleland, A. N. Bi-directional conversion between microwave and optical frequencies in a piezoelectric optomechanical device. *Appl. Phys. Lett.* **109**, 033107 (2016).
62. Gavartin, E., Verlot, P. & Kippenberg, T. J. A hybrid on-chip optomechanical transducer for ultrasensitive force measurements. *Nat. Nanotechnol.* **7**, 509–514 (2012).
63. Kimble, H. J. The quantum internet. *Nature* **453**, 1023–1030 (2008).
64. Kurizki, G. *et al.* Quantum technologies with hybrid systems. *Proc. Natl. Acad. Sci.* **112**, 3866–3873 (2015).

65. Zeuthen, E., Schliesser, A., Sørensen, A. S. & Taylor, J. M. Figures of merit for quantum transducers. *ArXiv161001099 Quant-Ph* (2016).
66. Takeda, K. *et al.* Electro-mechano-optical NMR detection. *ArXiv170600532 Phys. Physicsquant-Ph* (2017).
67. Tallur, S. & Bhave, S. A. A Silicon Electromechanical Photodetector. *Nano Lett.* **13**, 2760–2765 (2013).
68. Andrews, R. W. *et al.* Bidirectional and efficient conversion between microwave and optical light. *Nat. Phys.* **10**, 321–326 (2014).
69. Tsaturyan, Y., Barg, A., Polzik, E. S. & Schliesser, A. Ultracoherent nanomechanical resonators via soft clamping and dissipation dilution. *Nat. Nanotechnol.* **advance online publication**, (2017).
70. Fink, J. M. *et al.* Quantum electromechanics on silicon nitride nanomembranes. *Nat. Commun.* **7**, 12396 (2016).
71. Zou, C.-L., Han, X., Jiang, L. & Tang, H. X. Cavity piezomechanical strong coupling and frequency conversion on an aluminum nitride chip. *Phys. Rev. A* **94**, 013812 (2016).
72. Schliesser, A. & Kippenberg, T. J. Chapter 5 - Cavity Optomechanics with Whispering-Gallery Mode Optical Micro-Resonators. in *Advances In Atomic, Molecular, and Optical Physics* (ed. Paul Berman, E. A. and C. L.) **58**, 207–323 (Academic Press, 2010).
73. Xiong, C., Fan, L., Sun, X. & Tang, H. X. Cavity piezooptomechanics: Piezoelectrically excited, optically transduced optomechanical resonators. *Appl. Phys. Lett.* **102**, 021110 (2013).
74. Fong, K. Y., Fan, L., Jiang, L., Han, X. & Tang, H. X. Microwave-assisted coherent and nonlinear control in cavity piezo-optomechanical systems. *Phys. Rev. A* **90**, 051801 (2014).
75. Bochmann, J., Vainsencher, A., Awschalom, D. D. & Cleland, A. N. Nanomechanical coupling between microwave and optical photons. *Nat. Phys.* **9**, 712–716 (2013).
76. Tadesse, S. A. & Li, M. Sub-optical wavelength acoustic wave modulation of integrated photonic resonators at microwave frequencies. *Nat. Commun.* **5**, 5402 (2014).
77. Balram, K. C., Davanço, M. I., Song, J. D. & Srinivasan, K. Coherent coupling between radiofrequency, optical and acoustic waves in piezo-optomechanical circuits. *Nat. Photonics* **10**, 346–352 (2016).
78. Shumeiko, V. S. Quantum acousto-optic transducer for superconducting qubits. *Phys. Rev. A* **93**, 023838 (2016).
79. Okada, A. *et al.* Cavity optomechanics with surface acoustic waves. *ArXiv170504593 Cond-Mat Physicsphysics Physicsquant-Ph* (2017).
80. Balram, K. C. *et al.* Acousto-Optic Modulation and Optoacoustic Gating in Piezo-Optomechanical Circuits. *Phys. Rev. Appl.* **7**, 024008 (2017).
81. Meenehan, S. M. *et al.* Silicon optomechanical crystal resonator at millikelvin temperatures. *Phys. Rev. A* **90**, 011803 (2014).
82. Arrangoiz-Arriola, P. & Safavi-Naeini, A. H. Engineering interactions between superconducting qubits and phononic nanostructures. *Phys. Rev. A* **94**, 063864 (2016).
83. Gustafsson, M. V. *et al.* Propagating phonons coupled to an artificial atom. *Science* **346**, 207–211 (2014).
84. Černotík, O. & Hammerer, K. Measurement-induced long-distance entanglement of superconducting qubits using optomechanical transducers. *Phys. Rev. A* **94**, 012340 (2016).
85. Fang, K., Yu, Z. & Fan, S. Photonic Aharonov-Bohm Effect Based on Dynamic Modulation. *Phys. Rev. Lett.* **108**, 153901 (2012).
86. Xu, X.-W., Li, Y., Chen, A.-X. & Liu, Y. Nonreciprocal conversion between microwave and optical photons in electro-optomechanical systems. *Phys. Rev. A* **93**, 023827 (2016).
87. Fang, K. *et al.* Generalized non-reciprocity in an optomechanical circuit via synthetic magnetism and reservoir engineering. *Nat. Phys.* **13**, 465–471 (2017).
88. Fang, K., Matheny, M. H., Luan, X. & Painter, O. Optical transduction and routing of microwave phonons in cavity-optomechanical circuits. *Nat. Photonics* **10**, 489–496 (2016).
89. Li, J., Lee, H. & Vahala, K. J. Microwave synthesizer using an on-chip Brillouin oscillator. *Nat. Commun.* **4**, ncomms3097 (2013).

90. Benevides, R., Santos, F. G. S., Luiz, G. O., Wiederhecker, G. S. & Alegre, T. P. M. Ultrahigh-Q optomechanical crystals cavities fabricated on a CMOS foundry. *ArXiv170103410 Cond-Mat Physicsphysics* (2017).
91. Marinis, T. F., Soucy, J. W., Lawrence, J. G. & Owens, M. M. Wafer level vacuum packaging of MEMS sensors. in *Proceedings Electronic Components and Technology, 2005. ECTC '05.* 1081–1088 Vol. 2 (2005). doi:10.1109/ECTC.2005.1441406
92. Parker, L. Adiabatic Invariance in Simple Harmonic Motion. *Am. J. Phys.* **39**, 24–27 (1971).
93. Povinelli, M. L. *et al.* High-Q enhancement of attractive and repulsive optical forces between coupled whispering-gallery-mode resonators. *Opt. Express* **13**, 8286–8295 (2005).
94. Johnson, S. G. *et al.* Perturbation theory for Maxwell's equations with shifting material boundaries. *Phys. Rev. E* **65**, 066611 (2002).

Acknowledgements

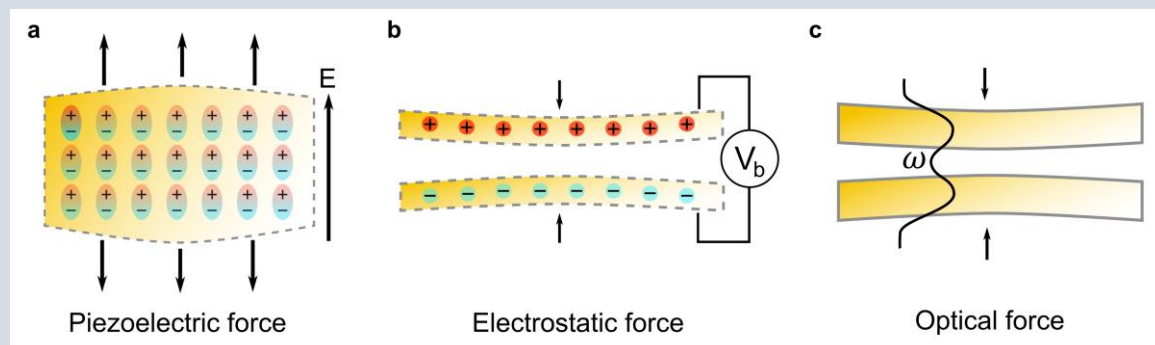
The authors gratefully acknowledge interesting discussions with N. Calabretta, M. Cotrufo, R.W. van der Heijden, M. Petruzzella, R. Stabile, K. Williams, Z. Zobenica, E. Verhagen, P. Lodahl, S. Stobbe, and K. Srinivasan. The research leading to these results was funded by the European Union's Horizon 2020 research and innovation programme (ERC project Q-CEOM, grant agreement no. 638765 and FET-proactive project HOT, grant agreement no. 732894), a starting grant and a postdoctoral grant from the Danish Council for Independent Research (grant number 4002-00060 and 4184-00203), the Dutch Technology Foundation STW, Applied Science Division of NWO, the Technology Program of the Ministry of Economic Affairs under projects Nos. 10380 and 12662 and the Dutch Ministry of Education, Culture and Science under Gravity program "Research Centre for Integrated Nanophotonics".

Competing interests

The authors declare no competing financial interests.

Box 1 | Optical and electrical forces.

Here we discuss in more detail the optical and electrical forces relevant for the operation of NOEMS. Both forces fall under the general theory of Lorentz forces and can be calculated from the Maxwell stress tensor, provided that the electric field E and the magnetic field B are known everywhere in space and that there are no moving charges. However, this requires involved numerical analysis and often is of little practical use. It is much more convenient to treat these forces using the work-energy formalism, where the energy U stored in an electrostatic or optical field gives rise to a force whenever a mechanical motion alters such energy, i.e. $F = -dU/dx$. In non-magnetic materials, only the energy in the electric field is coupled to motion, as the magnetic permeability is constant throughout the structure.

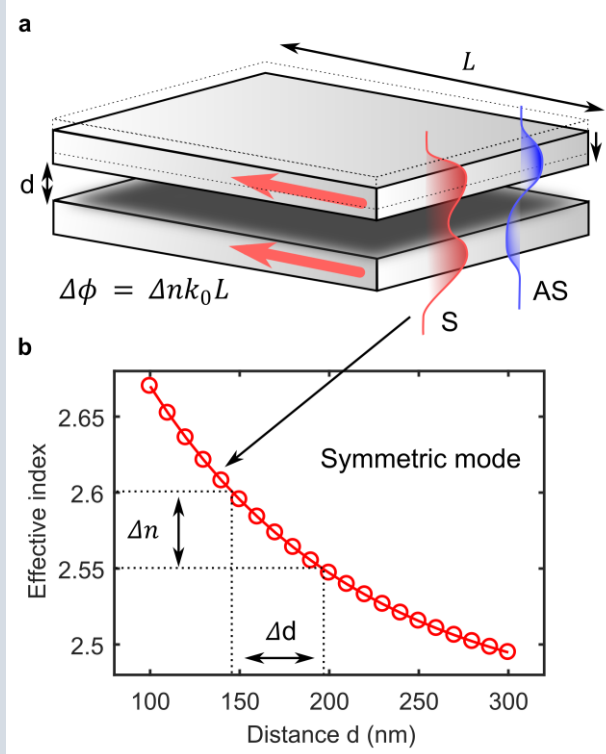


In a system of fixed charges subject to an external field, as in a piezoelectric material (a), the energy can be written as the sum of dipole energies, which depend on distance between charges, corresponding to a force (inverse piezoelectric effect). In the case of an electromechanical capacitor

with metal plates (b), $U = \frac{1}{2}QV$ (Q and V being the charge on the plates and the voltage between them) the force can be written as: $F = \frac{1}{2}Q \left. \frac{dV}{dx} \right|_Q = \frac{1}{2}V^2 \frac{dC}{dx}$, where $C(x)$ is the displacement-dependent capacitance, which is easy to evaluate numerically. For example, in a parallel-plate capacitor of area $10 \times 10 \mu\text{m}^2$, with plates spaced by 200 nm, the force equals ~ 100 nN under a voltage of 2 V. In the case where energy can be exchanged between the electric and the magnetic field, as in a LC circuit or for optical cavities, the effect of the moving capacitor on the circuit dynamics must be accounted for. However, in the adiabatic limit, the energy exchange, occurring at the electromagnetic resonance frequency ω , is much faster than the timescales of mechanical motion produced by the force, so that the electromagnetic system can be seen as a resonator whose frequency is affected by the motion (parametric coupling) (c). This guarantees that U/ω (which corresponds to the number of photons N_{ph}) is an invariant (see for example Ref⁹²). In this case the force can be written⁹³ as $F = -N_{ph} \hbar \frac{d\omega}{dx}$ (where \hbar is the reduced Planck constant). This general expression links optical forces to the opto-mechanical coupling factor $d\omega/dx$ which can be calculated from the solution to the Maxwell equations in the optical case⁹⁴. In coupled-nanobeam PhC cavities (Fig. 1b), $\frac{d\omega}{dx} \sim 2\pi \cdot 100 \text{ GHz/nm}$, corresponding to a force of ~ 66 fN/photon. Note that in both the electrostatic and optomechanical (adiabatic) case the force can be written as $|F| = \frac{U}{L^{eff}}$, where the effective coupling lengths²⁷ $L_{ES}^{eff} = \left| \frac{1}{C} \frac{dC}{dx} \right|^{-1}$, $L_{OM}^{eff} = \left| \frac{1}{\omega} \frac{d\omega}{dx} \right|^{-1}$ are of order of the dimensions over which the fields are confined (e.g. gap between plates of the capacitor or mirror spacing in a Fabry-Perot cavity) and therefore in the μm - and sub- μm range for NOEMS for both electrostatic and optomechanical actuation. While charges can be confined in sub- μm structures with negligible leakage, it is much more difficult to simultaneously achieve high confinement and small loss rate (thereby high stored energy) for optical fields, so that electrostatic forces tend to be much larger than optical forces for typical operating conditions.

Box 2 | Example of effective electro-optic interaction in NOEMS: parallel waveguides.

The mechanical deformation of nanophotonic waveguides can be engineered to provide a very strong effective electro-optic interaction in any type of material, including silicon. Here we discuss a specific example, which is at the basis of many NOEMS: a gap-controlled phase shifter. It comprises two closely-spaced parallel waveguides whose distance can be controlled electro-mechanically (a). At the core of the phase shifter operation is the splitting of modes into symmetric (S) and anti-symmetric (AS) (or bonding and anti-bonding) supermodes, originating from the evanescent coupling of the individual waveguides. The distance d between the waveguides determines the overlap of the evanescent field of one waveguide with the other one, and therefore the coupling strength μ and the difference in propagation constants between these supermodes according to an exponential law $\propto \exp(-\gamma d)$, where γ is the spatial decay of the evanescent field³⁵. The gap-dependent splitting translates directly into a variable propagation constant (or effective refractive index) for the two supermodes.



The plot in (b) shows the effective index change as a function of the distance for two 160-nm-thick semiconductor slabs ($n=3.4$) at a wavelength of 1550 nm. The use of electrostatic forces for the motion can lead to a very large electro-optic effect which could be used for phase modulation and switching.

Phase shifters are widely used in photonics, as they form the basis of tuneable lasers and Mach-Zehnder modulators. Phase differences also determine the output of directional couplers, arrayed waveguide gratings and phased arrays. All these systems rely on the controlled variation of optical length resulting in a phase change of $\Delta\phi = \Delta n k_0 L = \pi$, where $k_0 = 2\pi/\lambda$ is the wavenumber in vacuum and L the device length. The relevant figure of merit for a phase shifter is the voltage V_π required to obtain a π -phase shift in a given length. In a NOEMS gap-controlled shifter, a modulation up to $\Delta n_{eff} = 0.05$ and thereby π phase shifts in a 15 μm -long waveguide with a distance change of less than 50 nm are possible (b). These displacements are typically obtained with less than 10 V in standard capacitors or p-i-n junctions (i.e. the product $V_\pi L \sim 10^{-2} \text{ V} \cdot \text{cm}$). The electrostatic nature of the actuation also implies fJ-range actuation energy and nW-level static power dissipation. In crystals such as lithium niobate or PLZT, featuring a relatively high electro-optic coefficient, the small index modulation 10^{-4} implies cm-range interaction lengths and $V_\pi L$ products two to three order of magnitude larger than those achievable in NOEMS. In silicon, where the electro-optic effect is absent, static phase modulation is commonly achieved using the thermo-optic effect, which requires large static power dissipation in the range of tens of mW. While electro-optic modulators provide < 1 ns response times, we note that a waveguide with the dimensions discussed above has resonances in the 1-10 MHz range, thus limiting the response time just below the μs .